Rapid Communication

J. Biochem. **135**, 279–283 (2004)
DOI: 10.1093/jb/mvh033

First Determination of the Inhibitor Complex Structure of Human Hematopoietic Prostaglandin D Synthase

Tsuyoshi Inoue[1,2], Yousuke Okano[1], Yuji Kado[1], Kousuke Aritake[3], Daisuke Irikura[3], Nobuko Uodome[3], Nobuo Okazaki[1], Shigehiro Kinugasa[1], Hideyuki Shishitani[1], Hiroyoshi Matsumura[1], Yasushi Kai[*,1] and Yoshihiro Urade[*,3]

[1]Department of Materials Chemistry, Graduate School of Engineering, Osaka University, Suita, Osaka 565-0871; [2]Structure and Function of Biomolecules Group, PRESTO, Japan Science and Technology Agency, 4-1-8 Honcho, Kawaguchi, Saitama; and [3]Department of Molecular Behavioral Biology, Japan Science and Technology Corporation, Osaka Bioscience Institute, Osaka 565-0874

Received December 17, 2003; accepted December 27, 2003

Hematopoietic prostaglandin (PG) D synthase (H-PGDS) is responsible for the production of PGD_2 as an allergy or inflammation mediator in mast and Th2 cells. We determined the X-ray structure of human H-PGDS complexed with an inhibitor, 2-(2′-benzothiazolyl)-5-styryl-3-(4′-phthalhydrazidyl) tetrazolium chloride (BSPT) at 1.9 Å resolution in the presence of Mg^{2+}. The styryl group of the inhibitor penetrated to the bottom of the active site cleft, and the tetrazole ring was stabilized by the stacking interaction with Trp104, inducing large movement around the α5-helix, which caused the space group of the complex crystal to change from $P2_1$ to $P1$ upon binding of BSPT. The phthalhydrazidyl group of BSPT exhibited steric hindrance due to the cofactor, glutathione (GSH), increasing the IC_{50} value of BSPT for human H-PGDS from 36.2 μM to 98.1 μM upon binding of Mg^{2+}, because the K_m value of GSH for human H-PGDS was decreased from 0.60 μM in the presence of EDTA to 0.14 μM in the presence of Mg^{2+}. We have to avoid steric hindrance of the GSH molecule that was stabilized by intracellular Mg^{2+} in the mM range in the cytosol for further development of structure-based anti-allergic drugs.

Key words: anti-allergic drug, hematopoietic prostaglandin D synthase, inhibitor complex, structure-based drug design, X-ray structure.

Abbreviations: PG, prostaglandin; H-PGDS, hematopoietic prostaglandin D synthase; BSPT, 2-(2′-benzothiazolyl)-5-styryl-3-(4′-phthalhydrazidyl) tetrazolium chloride; PGD_2, postaglandin D_2; GST, glutathione S-transferase; GSH, glutathione.

In the arachidonate cascade, prostaglandin D_2 (PGD_2) is a lipid mediator (*1*, *2*) that functions as an allergy and inflammation mediator (*3*, *4*), and is produced by mast (*3*) and Th2 (*5*) cells in a variety of human tissues. PGD_2 is formed from PGH_2, a common precursor for all PGs and thromboxanes, by hematopoietic PGD synthase (H-PGDS) (*6*, *7*) in mast (*8*) and Th2 (*5*) cells.

Overproduction of PGD_2 exacerbates asthmatic reactions, as shown by an ovalbumin-challenged asthma model of human lipocalin-type PGDS- or H-PGDS-transgenic mice (*9*). On the other hand, asthmatic reactions are weak in prostanoid-specific G-protein coupled receptor (DP receptor) gene-knockout mice (*4*). The DP receptor, specific for PGD_2, is constitutively expressed in human basophils and eosinophils, and is induced in pulmonary and airway epithelial cells on allergic inflammation (*4*). PGD_2 also acts as a ligand for an orphan receptor, CRTH2 (*10*), which is expressed in human Th2 cells, eosinophils and basophils, and mediates the chemotaxis of these cells with PGD_2. Aerosolized PGD_2 increased not only the numbers of eosinophils, lymphocytes, and macrophages, but also the levels of IL-4 and IL-5 in bronchoalveolar lavage fluid. It has also been found to accelerate Th2 type inflammation through induction of macrophage-derived chemokine (*11*). Therefore, the PGD_2 produced by H-PGDS in human mast cells and Th2 cells is considered to accelerate allergic and inflammatory reactions by stimulating DP and CRTH2 receptors in autocrine and paracrine manners, respectively. Thus, human H-PGDS is a promising target for the design of anti-allergic and anti-inflammatory drugs.

We previously demonstrated that H-PGDS is the first identified vertebrate homologue of the σ-type of GSH S-transferase (GST) (*12–14*), and also reported the 2.3 Å resolution structure of rat H-PGDS (*12*). We then determined the crystal structures of Ca^{2+}- and Mg^{2+}-bound human H-PGDS with the space group of $P2_1$, finding that recombinant human H-PGDS was activated by Mg^{2+} with an EC_{50} value of 50 mM. The affinity of human H-PGDS for GSH was increased more than 4-fold in the presence of Mg^{2+} (K_m = 0.14 mM), compared with in the presence of EDTA (K_m = 0.60 mM) (*15*). We thus started to determine the structure of the inhibitor complex of human H-PGDS to obtain structural information that may be helpful for the further development of anti-allergic drugs.

The isolation and purification of human H-PGDS were carried out by the methods reported previously (*14*, *15*).

*To whom correspondence should be addressed. Dr. Yoshihiro Urade, Tel: +81-6-6872-4851, Fax: +81-6-6872-2841, E-mail: uradey@obi.or.jp; or Dr. Yasushi Kai, Tel: +81-6-6879-7410, Fax: +81-6-6879-7409, E-mail: kai@chem.eng.osaka-u.ac.jp

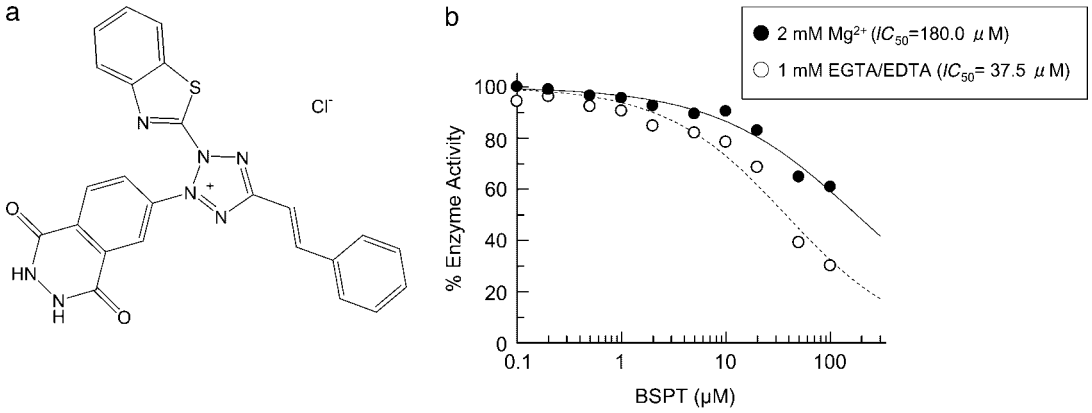

Fig. 1. **The structure of 2-(2′-benzothiazolyl)-5-styryl-3-(4′-phthalhydrazidyl) tetrazolium chloride (BSPT) (a), and inhibition of PGDS activity as a function of the concentration of BSPT added (b).** The concentrations of BSPT up to 100 μM were examined in the presence of 1 mM EDTA or 2 mM Mg^{2+}.

H-PGDS activity was measured, up to 40 μM [1-^{14}C] PGH_2, in a solution comprising 0.1 M Tris-HCl (pH 8.0), 2 mM GSH, and 0.1 mg/ml IgG, in the presence of EDTA/EGTA or Mg^{2+} with various concentrations of the inhibitor, BSPT (*12*). Fig. 1b shows the results of inhibition of the enzymatic activity of human H-PGDS by BSPT. The IC_{50} value was determined to be 36.2 μM in the presence of EDTA, however, it was 98.1 μM in the presence of Mg^{2+}.

Complex crystals of human H-PGDS with BSPT were obtained by a soaking method involving native crystals obtained as previously reported (*14*, *15*). Namely, crystals of H-PGDS were first grown by the hanging-drop vapor-diffusion method with PEG6000 as the precipitant at 20°C in the presence of 5 mM Mg^{2+}, and the native crystals were then soaked in the precipitant solution with a saturating concentration of BSPT for 2 weeks.

The X-ray diffraction data set for the BSPT-bound complex was collected at SPring-8 beam-line 40B2 (Table 1). The data were integrated and scaled with *DENZO* and *SCALEPACK* (*16*), and structure analysis was carried out using the Mg^{2+}-bound native structure as the starting model with the molecular replacement program of *AMORE* (*17*). Model re-building was performed with *O* (*18*) and *TURBO-FRODO* (*19*), and the complex structure was refined with the *CNS* program (*20*): 5% of the reflections were set aside for R_{free} calculations (*21*). Ordered water molecules were included by selecting peaks based on F_{obs}–F_{calc} difference Fourier maps contoured at 2.5σ, and $2F_{obs}$–F_{calc} maps contoured at 1.2σ. The quality of the models was assessed by means of Ramachandran plots, and analysis of the model geometry was carried out with *PROCHECK* (*22*). The results of data collection and refinement of the complex structure with BSPT are summarized in Table 1.

We obtained triclinic *P*1 crystals of human H-PGDS in the presence of Mg^{2+} and BSPT at pH 8.4, and determined the structure at 1.9 Å resolution. The complex crystals contained 2 dimer molecules, Mol-A and Mol-D, and Mol-C and Mol-B, in an asymmetric unit with a *P*1 lattice like the Mg^{2+}-bound native crystals; however, the packing structure was different from that of the Mg^{2+}-bound native form (Fig. 2a). In particular, the local two-fold axis of the second dimer, Mol-B and Mol-C, in the complex crystal was different from that in the native one by 169 degrees. Mol-A and Mol-B on the outside and Mol-C and Mol-D on the inside of the asymmetric unit showed small averaged root mean square (r.m.s.) deviations of 0.13 Å and 0.05 Å, respectively, for all the Cα carbon atoms. On the other hand, the r.m.s. deviations for superimposing of other combinations were calculated to range from 0.41 to 0.42 Å.

Table 1. **Data collection and refinement statistics for the H-PGDS complexed with BSPT.**

Data set	
Metal ion	Mg^{2+}
Space group	*P*1
X-ray source	SPring-8 BL40B2
Detector	Quantum 4R
Max resolution (Å)	1.9
No. of flames	250
Oscillation angles (deg.)	1.2
Measured/Unique reflections	426,168/67,589
Redundancy	6.3
Cell dimentions (Å, deg.)	a = 47.3, b = 49.2, c = 94.5
	α = 93.25, β = 89.98, γ = 90.01
Completeness (%)	95.8 (92.7)
Mean <*I*/sigma-*I*>	10.5
R_{merge}[a] (%)	6.3 (25.4)
Refinement statistics	
Resolution range (Å)	35.1–1.90
No. of GSH/BSPT	4/4
No. of water/glycerol	1462/6
R_{cryst}[b] (%)/R_{free}[c] (%)	19.5/21.5
Average B-factor (Å^2)	
GSH/BSPT	32.6/37.3
Stereochemistry	
Favorable/Allowed regions (%)	94.0/6.0
*R*msd bonds (Å)/angles (deg.)	0.008/1.1

Values in parentheses refer to outermost shells (1.97–1.90 Å). [a]$R_{merge} = \Sigma_j\Sigma_h |I_{hj} - \langle I_h \rangle| / \Sigma_j\Sigma_h \langle I_h \rangle$. [b]$R_{cryst} = \Sigma ||Fo| - |Fc|| / \Sigma|Fo|$ calculated from 95% of the data, which were used during the course of the refinement. [c]$R_{free} = \Sigma ||Fo| - |Fc|| / \Sigma|Fo|$, calculated from 5% of the data, which were used during the course of the refinement.

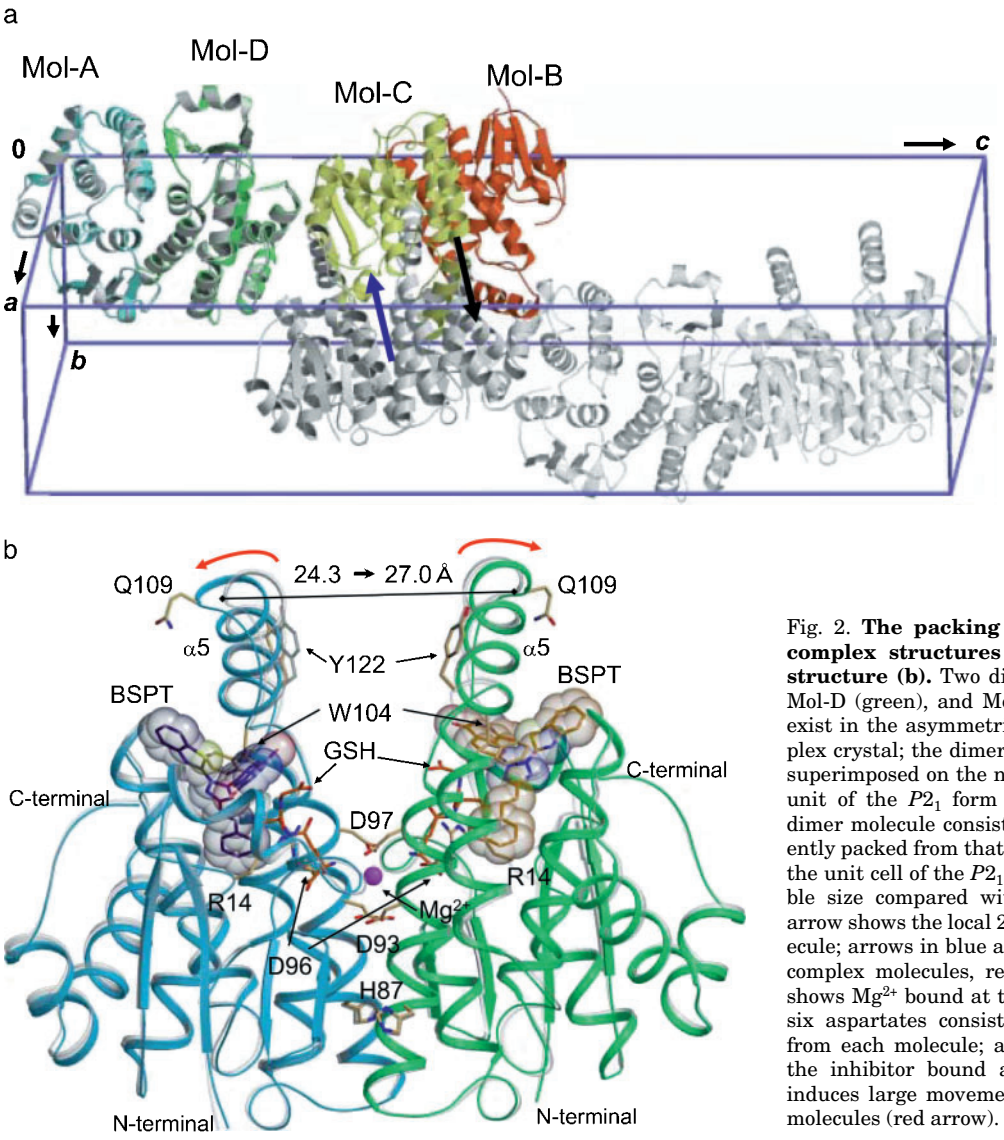

Fig. 2. **The packing structure (a), and the dimer complex structures superimposed on the native structure (b).** Two dimer molecules, Mol-A (cyan) and Mol-D (green), and Mol-C (yellow) and Mol-B (orange), exist in the asymmetric unit of the *P*1 form of the complex crystal; the dimer consisting of Mol-A and Mol-D is superimposed on the native structure of the asymmetric unit of the $P2_1$ form (gray), showing that the second dimer molecule consisting of Mol-B and Mol-C is differently packed from that of the native form. The box shows the unit cell of the $P2_1$ form in the native crystal at double size compared with the complex crystal, and the arrow shows the local 2-fold axis of the second dimer molecule; arrows in blue and black represent the native and complex molecules, respectively (a). The magenta ball shows Mg^{2+} bound at the dimer interface surrounded by six aspartates consisting of Asp93, Asp96 and Asp97 from each molecule; and the space-filling model shows the inhibitor bound at the active site. The inhibitor induces large movement of the α5-helices in the dimer molecules (red arrow).

The dimer formation of human H-PGDS was essentially the same as those of other GSTs, *i.e.* rat and human H-PGDS (*12*, *15*). However, superimposing of the Mg^{2+}-bound dimer structures of the complex and the native form revealed that a remarkable structural change had occurred around the α5-helix in each monomer in the dimer structure (Fig. 2b). The r.m.s. deviations of the Cα carbon atoms of Mol-A and Mol-D between the complex and the native form were 0.42 and 0.58 Å, respectively. Induced-fitting of the α4- and α5-helices obviously occurred upon the binding of BSPT in the presence Mg^{2+}, increasing the distance between the Cα(Gln109) carbon atoms of Mol-A and Mol-D from 24.3 to 27.0 Å (Fig. 2b). This movement broke the hydrogen bond between Tyr122 in Mol-A and His87 in the neighboring molecule, which had previously been found in Ca^{2+}- or Mg^{2+}-bound native crystals. This could have been the cause of the change of the space group from $P2_1$ to *P*1.

The complex structure, consisting of a βαβαββα motif in the N-terminal domain and four α-helices in the C-terminal domain, was similar to those of the Ca^{2+}- and Mg^{2+}-bound native structures (*15*). The inhibitor molecule BSPT bound in the putative catalytic pockets, which consist of Tyr8, Arg14, Trp104, Lys112, Tyr152, Cys156, and Lys198 (Fig. 3a). Previously, the active site pockets of H-PGDS were defined by Kanaoka *et al*. (*12*), Trp104, Met11, Ala105, Leu199 and GSH forming Pocket 1, in which the tetrazole ring of BSPT is located and in a stacking interaction with Trp104 (Fig. 3b). The distance between the indole and tetrazole rings was determined to be 3.65 Å in the complex structure. Both the benzothiazolyl and phthalhydrazidyl groups of BSPT were located in the pocket, the former being in a van der Waals interaction with Met11 and Leu199, and the latter with Gln36. However, the glycine part of GSH exhibited steric hindrance due to the phthalhydrazidyl group of BSPT, being 1.7 Å apart from the inhibitor (Fig. 3a). Along with movement of the glycine part of GSH, Gln36 and Trp39 residues exhibited conformational changes, resulting the structural changes in the N-terminal domain of H-PGDS. Gly13, Arg14, Met99 and Tyr152 formed Pocket 2, in which the styryl group of the inhibitor penetrated to the

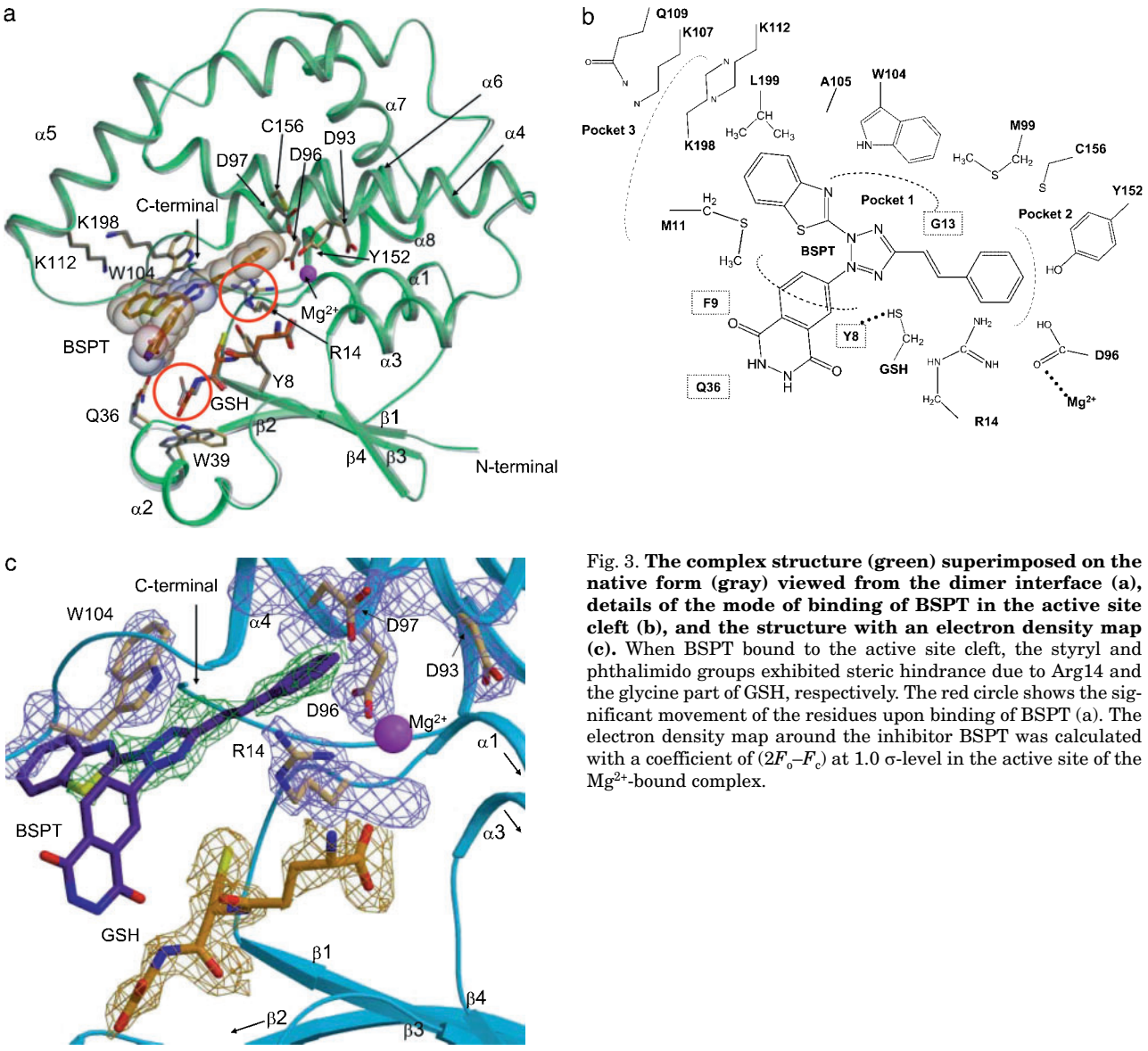

Fig. 3. **The complex structure (green) superimposed on the native form (gray) viewed from the dimer interface (a), details of the mode of binding of BSPT in the active site cleft (b), and the structure with an electron density map (c).** When BSPT bound to the active site cleft, the styryl and phthalimido groups exhibited steric hindrance due to Arg14 and the glycine part of GSH, respectively. The red circle shows the significant movement of the residues upon binding of BSPT (a). The electron density map around the inhibitor BSPT was calculated with a coefficient of $(2F_o–F_c)$ at 1.0 σ-level in the active site of the Mg^{2+}-bound complex.

bottom of the pocket. The Arg14 residue was 1.85 Å apart from the styryl group of the inhibitor. It was previously proposed that Pocket 3 contained the conserved Lys107, Gln109, Lys112 and Lys198 residues that recognize the α-chain of the substrate PGH_2, however, there is no interaction with BSPT in Pocket 3. Although the electron densities for both the GSH and BSPT molecules were obtained for all four molecules in the complex (Fig. 3c), the corresponding densities for both the benzothiazolyl and phthalhydrazidyl rings were poor due to there being no hydrogen bond with the main or side chains, allowing free rotation of these functional groups. Free rotation of these functional groups of BSPT may inhibit the binding of GSH. The affinity of GSH for the enzyme was increased by more than 4-fold upon binding of Mg^{2+}. This may be the reason why the IC_{50} value of BSPT increased from 36.2 to 98.1 mM in the presence of Mg^{2+}.

The further development of anti-inflammatory or anti-allergic inhibitors should be performed without steric hindrance by GSH, since H-PGDS is activated by intracellular Mg^{2+} in the mM order in the cytosol in our Th2 and mast cells.

The atomic coordinates and structure factors (code 1V40) have been deposited in the Protein Data Bank, Research Collaboratory for Structural Bioinformatics, Rutgers University, New Brunswick, NJ.

We thank Dr. Keiko Miura of JASRI for the valuable help with data collection with synchrotron radiation at BL40B2, SPring-8. We also express our appreciation to Emeritus Prof. Osamu Hayaishi, Osaka Bioscience Institute, for his generous support of this study. This study was funded by the PRESTO (T.I.) and CREST (Y.U.) projects, Japan Science and Technology Corporation, and was a part of the "Applied Research Pilot Project for the Industrial Use of Space" promoted by JAXA and the Japan Space Utilization Promotion Center, the National Project on Protein Structural and Functional Analyses, the New Energy and Industrial Technology Development Organization (NEDO), the Handai Frontier Research Center, and Osaka City.

REFERENCES

1. Giles, H. and Leff, P. (1988) The biology and pharmacology of PGD2. *Prostaglandins* **35**, 277–300
2. Ito, S., Narumiya, S., and Hayaishi, O. (1989) Prostaglandin D2: a biochemical perspective. *Prostaglandins Leukot Essent Fatty Acids* **37**, 219–234
3. Lewis, R.A., Soter, N.A., Diamond, P.T., Austen, K.F., Oates, J.A., and Roberts, L.J., 2nd (1982) Prostaglandin D2 generation after activation of rat and human mast cells with anti-IgE. *J. Immunol.* **129**, 1627–1631
4. Matsuoka, T., Hirata, M., Tanaka, H., Takahashi, Y., Murata, T., Kabashima, K., Sugimoto, Y., Kobayashi, T., Ushikubi, F., Aze, Y., Eguchi, N., Urade, Y., Yoshida, N., Kimura, K., Mizoguchi, A., Honda, Y., Nagai, H., and Narumiya, S. (2000) Prostaglandin D2 as a mediator of allergic asthma. *Science* **287**, 2013–2017
5. Nagata, K., Tanaka, K., Ogawa, K., Kemmotsu, K., Imai, T., Yoshie, O., Abe, H., Tada, K., Nakamura, M., Sugamura, K., and Takano, S. (1999) Selective expression of a novel surface molecule by human Th2 cells *in vivo*. *J. Immunol.* **162**, 1278–1286
6. Urade, Y. and Hayaishi, O. (2000) Prostaglandin D synthase: structure and function. *Vitam Horm* **58**, 89–120
7. Kanaoka, Y. and Urade, Y. (2003) Hematopoietic prostaglandin D synthase. *Prostaglandins Leukot Essent Fatty Acids* **69**, 163–167
8. Urade, Y., Ujihara, M., Horiguchi, Y., Igarashi, M., Nagata, A., Ikai, K., and Hayaishi, O. (1990) Mast cells contain spleen-type prostaglandin D synthetase. *J. Biol. Chem.* **265**, 371–375
9. Fujitani, Y., Kanaoka, Y., Aritake, K., Uodome, N., Okazaki-Hatake, K., and Urade, Y. (2002) Pronounced eosinophilic lung inflammation and Th2 cytokine release in human lipocalin-type prostaglandin D synthase transgenic mice. *J. Immunol.* **168**, 443–449
10. Hirai, H., Tanaka, K., Yoshie, O., Ogawa, K., Kenmotsu, K., Takamori, Y., Ichimasa, M., Sugamura, K., Nakamura, M., Takano, S., and Nagata, K. (2001) Prostaglandin D2 selectively induces chemotaxis in T helper type 2 cells, eosinophils, and basophils *via* seven-transmembrane receptor CRTH2. *J. Exp. Med.* **193**, 255–261
11. Honda, K., Arima, M., Cheng, G., Taki, S., Hirata, H., Eda, F., Fukushima, F., Yamaguchi, B., Hatano, M., Tokuhisa, T., and Fukuda, T. (2003) Prostaglandin D2 reinforces Th2 type inflammatory responses of airways to low-dose antigen through bronchial expression of macrophage-derived chemokine. *J. Exp. Med.* **198**, 533–543
12. Kanaoka, Y., Ago, H., Inagaki, E., Nanayama, T., Miyano, M., Kikuno, R., Fujii, Y., Eguchi, N., Toh, H., Urade, Y., and Hayaishi, O. (1997) Cloning and crystal structure of hematopoietic prostaglandin D synthase. *Cell* **90**, 1085–1095
13. Meyer, D.J. and Thomas, M. (1995) Characterization of rat spleen prostaglandin H D-isomerase as a sigma-class GSH transferase. *Biochem. J.* **311**, 739–742
14. Kanaoka, Y., Fujimori, K., Kikuno, R., Sakaguchi, Y., Urade, Y., and Hayaishi, O. (2000) Structure and chromosomal localization of human and mouse genes for hematopoietic prostaglandin D synthase. Conservation of the ancestral genomic structure of sigma-class glutathione S-transferase. *Eur. J. Biochem.* **267**, 3315–3322
15. Inoue, T., Irikura, D., Okazaki, N., Kinugasa, S., Matsumura, H., Uodome, N., Yamamoto, M., Kumasaka, T., Miyano, M., Kai, Y., and Urade, Y. (2003) Mechanism of metal activation of human hematopoietic prostaglandin D synthase. *Nat. Struct. Biol.* **10**, 291–296
16. Otwinowski, Z.M., W. (1993) Data Collection and Processing in *Proceedings of the CCP4 Study Weekend* (Sawyer, L., Issacs, N., and Bailey, S., eds.) 56–62, Science and Engineering Research Council (England) Daresbury Lab., Warrington, U.K.
17. Navaza, J. (2001) Implementation of molecular replacement in AMoRe. *Acta Cryst.* **D57**, 1367–1372
18. Jones, T.A., Zou, J.Y., Cowan, S.W., and Kjeldgaard (1991) Improved methods for building protein models in electron density maps and the location of errors in these models. *Acta Cryst.* **A47**, 110–119
19. Jones, T.A. (1985) Diffraction methods for biological macromolecules. Interactive computer graphics: FRODO. *Methods Enzymol.* **115**, 157–171
20. Brünger, A.T., Adams, P.D., Clore, G.M., DeLano, W.L., Gros, P., Grosse-Kunstleve, R.W., Jiang, J.S., Kuszewski, J., Nilges, M., Pannu, N.S., Read, R.J., Rice, L.M., Simonson, T., and Warren, G.L. (1998) Crystallography & NMR system: A new software suite for macromolecular structure determination. *Acta Cryst.* **D54**, 905–921
21. Brünger, A.T. (1992) Free R value: a novel statistical quantity for assessing the accuracy of crystal structures. *Nature* **355**, 472–475
22. Laskowsky (1993) PROCHECK: a program to check the stereochemical quality of protein structures. *J. Appl. Crystallogr.* **26**, 283–291